

RESULTS OF UNIAXIAL AND BIAXIAL TESTS ON RIVETED FUSELAGE  
LAP JOINT SPECIMENS

H. Vlieger  
National Aerospace Laboratory NLR  
Amsterdam, The Netherlands

113075

## INTRODUCTION

In the USA uniaxial fatigue tests were carried out for the FAA on riveted lap joint specimens to study the effect of various lap joint parameters on fatigue life and the occurrence of MSD. These tests were carried out by Arthur D. Little Co. (ADL) and the Fatigue Technical Institute (FTI). The parameters considered and their levels selected for these tests are shown in Table 1. Figure 1 gives some details of the design of the tested panel configurations. The panels were provided with tear straps and a longitudinal stiffener because the specimens had to be representative for fuselage longitudinal lap joints. The results of these tests are compiled in Ref.1. Considering MSD it was found from these tests that the stress level and the rivet spacing were the most important lap splice parameters.

As part of an FAA-NLR collaborative programme on structural integrity of ageing aircraft NLR carried out fatigue tests on riveted lap joint specimens of similar design as those tested by ADL/FTI, but now both uniaxial and biaxial fatigue tests were performed. The encircled values in Table 1 were chosen for the levels of the parameters in the NLR testing programme. This investigation was sponsored by the FAA. In this paper the experimental results obtained are presented.

## DESCRIPTION OF TESTING PROGRAMME

Table 2 shows the matrix of the testing programme carried out by NLR. Two stress levels and two rivet spacings were chosen as parameters in these tests resulting in 4 groups of specimens. All specimens had a skin thickness of 0.05 inch. The other panel characteristics were taken similar to those of the ADL/FTI baseline design (see Table 1). Only the panel widths were taken equal to 14 inches instead of 12 inches (see figure 2) to allow bonding of the clamping arms of the biaxial specimens alongside the tear straps (see next chapter). Further, apart from two specimens in group no 4, the longitudinal stiffener on the lap joint was missing. In each group of specimens the uniaxial tests were carried out in duplicate and the biaxial tests in triplicate. In total 22 specimens were tested (10 uniaxial + 12 biaxial specimens, see Table 2).

The main objective of the biaxial testing programme was to study possible effects of biaxial loading on fatigue life and occurrence of MSD with respect to results of uniaxial tests on lap joints of similar design. Further, comparison of the NLR and the ADL/FTI test results of panels of similar design was an objective.

## DESCRIPTION OF SPECIMENS

All specimens were delivered with a length of 36 inches. After delivery at NLR the specimens that were planned for uniaxial testing were provided in the clamping areas with aluminium tabs to prevent clamping failures (at either side of the sheet ends a 1 mm thick sheet was bonded for that purpose). Thereafter the hole pattern being present in the available plate fixtures of the testing machine (see below under Execution of Testing) was drilled in the specimens.

The specimens that were used for biaxial testing required a special treatment. To be able to run biaxial fatigue tests on specimens in which the lap joint is the fatigue critical area, the way of load introduction into the lap joint area is of paramount interest (Ref. 2). Figure 3 shows how this problem was solved: the biaxial loads were applied to the test section by means of load introducing arms consisting of unidirectional Aramid fibres embedded in epoxy resin. The composite parts of the load introducing arms were made separately by means of a lay-up of aramid prepreg layers. These parts were laid up in a mold and cured in this mold in one autoclave cycle. After curing the aramid parts were cold bonded to the specimen and to the end fixtures. To allow bonding of the horizontal arms to the biaxial specimens the width of all specimens was chosen equal to 14 inches thus leaving 1 inch of material outside of the tear straps free for bonding of the load introducing arms (see Figs. 2 and 3). The exploded view in Fig. 3 clearly shows the complexity of the manufacturing process of the load introducing arms of the biaxial specimens.

With regard to the longitudinal (sheet) stiffener being present on the ADL/FTI specimens (see Fig. 1) the following remarks can be made. It is to be expected that this stiffener will not have a significant effect on fatigue life and/or MSD. Further, in uniaxial testing the loading of this stiffener will not be very realistic: due to the restrained Poisson's constraint, in the tests the stiffener will be loaded in compression and consequently there will be load transfer from the skin to the stiffener. In reality this will hardly be the case. Finally, when considering biaxial testing the presence of this stiffener results in a more complex loading system because load has to be introduced in this stiffener to realise skin-stiffener compatibility during the test. On the basis of these arguments it was decided to omit this stiffener from the specimens in the NLR testing programme. However, in group no 4 (see Table 2) two extra test panels with this stiffener being present were included in the test matrix to study possible effects of this stiffener. These extra panels were tested uniaxially.

To allow comparison of the NLR results with those of Ref. 1 all specimens were manufactured in the USA by the same factory that delivered the specimens of Ref. 1, according to the same production drawings and the same aircraft production standards.

## EXECUTION OF TESTING

### Uniaxial tests

The uniaxial constant amplitude fatigue tests were carried out in a 900 kN Wolpert Amsler servo-hydraulic (MTS) testing machine. All tests were carried out under load control with an R-value (= ratio of minimum-to-maximum stress in a cycle) of 0.1 and at a frequency of 4 Hz (the same frequency that was used for the tests in Ref. 1). At that frequency no dynamic effects were experienced so that no special fixturing was required.

To check the correct alignment of the specimens during testing in order to obtain a symmetrical stress distribution across the specimen width, all specimens were provided with 4 (end load) strain gauges, i.e. 2 on the front side and 2 on the back side. The positions of these gauges were on the tear strap centrelines, 1 inch above the tear strap ends. After an acceptable alignment of the specimens was reached, prior to test initiation the panels were preloaded up to 1.33 times the maximum test load to simulate proof testing of the fuselage pressure cabin until 133% relief valve setting at delivery of the aircraft.

During the tests all rivet rows (at either side) were inspected frequently by means of a travelling binocular combined with a crack monitoring device (Sony Magnecsale EA-210). When during an inspection a crack was found, then the crosshair of the microscope was positioned successively at the extremities of that crack (i.e. at the rivet head edge and at the crack tip) and the distance between these positions was converted into mm's crack length by means of the displacement transducer in the crack monitoring device. The inspection frequency applied during the tests was based on experience about crack initiation lives gained during the execution of the testing programme. Initially inspections were carried out at rather small inspection intervals (say every 10,000 cycles) but these intervals increased during progress of the testing programme. After cracks were detected in a certain test, the inspections were carried out at smaller intervals to collect as much crack propagation data as possible from the test. Sometimes high frequency eddy current inspections (with a pencil probe) were carried out in support of the visual inspections.

### Biaxial tests

The biaxial constant amplitude fatigue tests were carried out in a biaxial fatigue testing frame containing two double-acting hydraulic actuators (see Fig.4). The actuators had a maximum capacity of 200 kN (horizontal actuator) and 100 kN (vertical actuator) and were controlled by close-loop servo systems. At the rod ends of the actuators double-bridge load cells were mounted. During the tests the ends of the four arms of the cruciform specimens were bolted to triangular plate fixtures which in turn were connected to (in length) adjustable tension rods. For each load system one of these tension rods was connected to an actuator load cell and the other to the structure of the test frame. The load systems of the test frame were controlled by a computerized signal generator and control system.

All specimens were subjected to "in-phase" biaxial stresses representing the fuselage pressurisation stress cycles with a biaxiality ratio (= ratio of longitudinal to hoop stress) of 0.5. The synchronisation of the phases of both load systems was controlled by the software of the control system.

All tests were carried out under load control with an R-value of 0.1 and at a frequency of 4 Hz. At that frequency no dynamic effects were experienced so that no special fixturing was required.

In a similar way as described for the uniaxial tests, the correct alignment of the specimens in the test frame during testing was obtained by means of strain gauges, but now in total 8 strain gauges were used, i.e. 4 for each load system. The positions of the strain gauges on the specimen are shown in Fig.4. The strain gauges of each load system were connected in a Wheatstone bridge. The alignment of the specimen in the test frame was carried out as follows. First, a static alignment was performed by adjusting the lengths of the tension rods in such a way that the panel centre was at the

centre of the test frame. Then, in both directions preloads of 1.33 times the maximum test loads occurring in a cycle were applied to the specimen. Finally, the alignment was further fine-tuned dynamically (starting at a low test frequency) by balancing the output of the Wheatstone bridges of both load systems.

The inspections during the tests were carried out in a similar way as described for the uniaxial tests with the exception that no travelling binocular combined with a crack monitoring device was available at the biaxial test frame. Instead the inspections were performed by means of a magnifying glass. In doubtful cases the visual inspections were supported by means of a high frequency eddy current inspection.

## TEST RESULTS

Table 3 gives a survey of the uniaxial and biaxial fatigue test results. The biaxial test results are presented in the shaded areas. These results will be discussed in more detail in the following chapter but a few general remarks can be made here on the basis of the data presented in this table.

Table 3 shows the number of kcycles at which the first cracks initiated in the critical (countersunk) rivet row of the lap joint and at the tear strap ends. The values in parentheses represent the percentages of panel failure lives at which this occurred. It is shown here that in almost all panels cracks initiated in the critical rivet row of the lap joint. The crack sizes that were assumed here to define crack initiation are shown at the bottom of the table. Generally also cracks arose in the skin at the tear strap ends due to high secondary bending stresses in these areas.

Further, the table presents the number of kcycles at which the panels failed together with their failure modes. Three panel failure modes are to be distinguished. Figure 5 illustrates how the three failure modes were defined:

- a panel failed in mode A when, after the initiation of cracks in the critical rivet row of the lap joint and linking up of these cracks until a continuous crack of sufficient length, the panel ultimately failed across the critical rivet row.
- failure in mode B occurred when the cracks in the skin at the tear strap ends became unstable before cracks in the lap joint had initiated and developed until a continuous crack of sufficient length. It is shown in Fig. 5 that at the moment of panel failure in the lap joint a crack of only two rivet spacings had developed.
- failure mode C is a combination of failure modes A and B. In this case one of the cracks being present in the skin at the tear strap ends became unstable as a consequence of fracture instability in the rivet row of the lap joint.

## DISCUSSION

The test results given in Table 3 were plotted in separate diagrams and will be discussed in more detail in the following sections.

## Crack initiation in lap joint area and fatigue lives

The diagram in Fig. 6a shows the crack initiation lives of the lap joints and the panel fatigue lives until failure. Further, the average failure life per specimen group and the failure modes are presented. The shaded bars refer to biaxial test results. The test results of the panels with longitudinal stiffeners were omitted.

It can be concluded from Fig. 6a that for each of the 4 groups of specimens in the uniaxial tests crack initiation in the critical rivet row of the lap joint generally started at a lower percentage of panel failure life than in the biaxial tests (see also data presented in Table 3).

Further, on an average in each group the uniaxially tested specimens showed the shortest failure lives. Finally, for both  $\sigma_{\max}$ -levels the specimens with the smaller rivet spacings showed the longest lives. All these observations particularly apply to the test results of groups 1 and 2, i.e. to the specimens tested at the lower  $\sigma_{\max}$ -values.

It has to be noted here that the uniaxially tested panels with a .75 inch rivet spacing all failed in mode B (i.e. across the tear strap ends, see Figure 5). This implies that the failure lives presented in Figure 6a for these panels are not representative for the fatigue lives of the lap joints but have to be considered as lower bounds thereof. This aspect has to be accounted for with regard to the conclusions drawn above about the fatigue lives found from the uniaxial and biaxial tests. For the uniaxially tested panels with a 1 inch rivet spacing in almost all cases (except for panel 3b-B; see Figure 6a) the fatigue lives of the lap joints determined the panel fatigue lives.

## Crack initiation in the skin at the tear strap ends and measures taken

During the execution of the testing programme both during the uniaxial and the biaxial tests generally cracks initiated in the skin from the rivet holes at the tear strap ends due to high secondary bending stresses in these areas. When this occurred corrective actions were taken in an attempt to increase the life of the panels to such an extent that cracks in the lap joint would have a chance either still to initiate or to develop further during the continuation of the test. This aspect is illustrated in the diagram of Fig. 6b.

At the bottom of the diagram in Fig. 6b the sequence of testing of the panels is shown. It has to be noted here that the biaxial tests were carried out after the uniaxial testing programme was completed.

During the execution of the uniaxial testing programme with the first tested specimen in which cracking at the tear strap ends occurred (specimen 3b-A, see Fig. 6b) no special measures were taken. With the next tested panel (specimen 3b-B, see Fig. 6b) the crack tips were stop-drilled with 5 mm  $\varnothing$  holes and these holes were cold worked. It has to be noted that such an action could not be applied before the cracks in the skin had passed the tear strap edges, implying that the crack had a length then of about 2 inches. Stop-drilling of these cracks was found to be not very effective: fairly soon after stop-drilling was carried out the panel failed in mode B across the stop-drilled cross section. Therefore with all other panels tested subsequently (both uniaxial and biaxial) the propagation of the cracks at the tear strap ends was stopped by applying a so-called "ball-indentation" process in the crack tip regions. During such a process residual compressive stresses are built up in the material at the crack tip by pressing a steel ball of 8 mm  $\varnothing$  in the material by means of a riveting hammer, meanwhile supporting the panel at the back side locally by means of a heavy piece of

metal. As is shown in Fig. 6b (see explanation given for specimen 2b-B) this crack arresting process had to be repeated a number of times during the test continuation because new cracks initiated at other locations or reinitiation of cracks at the hammered crack tips occurred later on. It can be seen from Fig. 6b that with the biaxial tests application of the BI-process appeared to be more effective than with the uniaxial tests: although with the biaxial tests the BI-process generally was applied for the first time before any crack initiation in the lap joint was discovered, all biaxially tested panels failed in mode A or mode C whereas in the uniaxially tested panels in which the BI-process was applied, all but one failed in mode B (panel 4c-A failed in mode C).

### Failure modes of panels

Comparing the results of the uniaxially and biaxially tested specimens, with regard to crack initiation and propagation in the critical row of the lap joint, a different behaviour was observed for both loading modes. This different behaviour was reflected in the failure modes of the panels.

In the uniaxially tested specimens crack initiation in the critical rivet row generally occurred more or less widespread, resulting in more separate cracks growing simultaneously, without showing obvious interaction.

In the biaxially tested specimens crack initiation in the critical rivet row generally occurred at two or more rivets positioned close together (but not necessarily next to one another) resulting in more cracks growing simultaneously and linking up of these cracks during test continuation. In these panels before panel failure a continuous crack (= a crack extending over one or more rivet spacings) was present in the critical row, extending over a large number (say 10) of rivet spacings.

Fig. 7 illustrates the crack initiation and propagation behaviour being typical for the uniaxially and biaxially tested panels. In the lower half of this figure this behaviour is shown for the critical rivet row as a function of the number of keycycles. It is shown that in the uniaxially tested panels cracks initiated at various locations along the rivet row and just before panel failure (i.e. after 213 keycycles) these cracks still had not linked up. At that moment a photograph was made of the area indicated in Fig. 7. This photograph (see Fig. 8) shows that cracks had propagated from adjacent rivets in opposite directions, more or less parallel to each other without showing linking up.

In the biaxially tested panel shown in Fig. 7 crack initiation remained limited to three adjacent rivets and linking up of these cracks occurred well in advance of panel failure.

Both with the uniaxially and biaxially tested panels, simultaneous with cracking of the critical rivet row of the lap joint, cracks also initiated in the sheet at the tear strap ends. Table 4 gives a survey of the crack lengths that were present in the panels at both locations just before panel failure together with the failure modes of the panels. The results of the biaxial tests are given in the shaded areas. It is clearly shown that all biaxial panels failed in mode A or mode C as a consequence of the large continuous cracks being present in the critical rivet row at the moment of panel failure (generally in these panels also rather large cracks were present at the tear strap ends, see Table 4). On the contrary, of the uniaxial panels that showed cracks at the tear strap ends, all but two (namely panels 3b-A and 4c-A which failed in mode C) failed in mode B because no cracks (or in one case a very small continuous crack) had developed in the critical rivet row during the test. Two of the uniaxial panels which did not show any crack initiation at the tear strap ends failed in mode A (panels 1b-A and 1b-B).

## Effect of longitudinal stiffener

The uniaxial specimens tested by ADL/FTI were all provided with a longitudinal stiffener (see Figure 1). In the NLR test programme this stiffener was missing with all specimens but two. These two extra specimens were incorporated in group 4 of the NLR test matrix (see Table 2) to allow examination of possible effects of this stiffener on panel behaviour. These extra specimens were tested uniaxially. The test results of these specimens (specimens 4c-A and 4c-B) are shown in the two lower lines of Table 3 and plotted in Fig. 6b. Apart from the longitudinal stiffener, the design and the test conditions of these panels were similar to those of panels 4b-A and 4b-B. Comparing the test results of the panels with and without this stiffener, no significant effect of the stiffener on panel behaviour could be established.

## Development of MSD

Table 5 shows the development of MSD during the last part of the test, i.e. after discovery during inspection of the first continuous crack in the critical rivet row of the lap joint. For obvious reasons only the data of the specimens that failed in mode A or mode C are presented in this table.

Columns 2 and 3 of the table present the number of kcycles tested until the inspection at which for the last time separate cracks were found to be present in the critical rivet row together with the number of rivets at which such cracks were found at that moment. The values in parentheses represent the corresponding percentages of panel failure lives.

The other columns of Table 5 present the number of kcycles at which continuous cracks were found during subsequent inspections together with the lengths of these cracks, expressed in number of rivet spacings. It has to be noted here that in almost all panels crack initiation only was observed in the critical countersunk rivet row. However, two specimens showed a different behaviour (viz., specimens 2a-B and 2a-C, see Table 5). In specimen 2a-B cracks developed in both critical rivet rows simultaneously. In specimen 2a-C crack initiation and propagation remained limited to the critical formed head rivet row, leading ultimately to failure across this row.

The results of Table 5 are plotted in Fig. 9. The moments of inspection are expressed in this figure as percentages of panel failure life. The inspections that represent the last inspection at which separate cracks were found are drawn dotted. The number of cracked rivets being present at that moment are given (see sketches in Fig. 9). The other levels in Fig. 9 represent the levels at which, successively, inspections were carried out and the numbers given at these levels pertain to the number of rivet spacings that were found to be cracked during these inspections.

It can be observed from Figure 9 that the last inspections at which separate cracks were found generally were carried out at levels above 95% of the panel failure lives and consequently development of these cracks across the rivet row ultimately leading to panel failure occurred in less than 5% of the life until failure.

## CONCLUSIONS

As part of an FAA-NLR collaborative programme on structural integrity of ageing aircraft, NLR carried out uniaxial and biaxial fatigue tests on riveted lap joint specimens being representative for application in a fuselage. All tests were constant amplitude tests with maximum stresses being representative for fuselage pressurization cycles and R-values of 0.1. The parameters selected in the testing programme were the stress level ( $\sigma_{\max} = 14$  and 16 ksi) and the rivet spacing (.75 and 1.0 inch). All specimens contained 3 rows of countersunk rivets, the rivet row spacing was 1 inch and the rivet orientation continuous.

From the test results the following conclusions can be drawn:

- i) Comparing the results of identical specimens it was found that in the uniaxial tests crack initiation in the critical (countersunk) rivet row generally started at a lower percentage of the panel failure life than in the biaxial tests. Further, averaged per group of specimens, the uniaxially tested specimens showed the shortest failure lives.
- ii) Independent of the loading mode, for both stress levels the specimens with the smaller rivet spacings showed the longest failure lives.
- iii) Crack initiation in the critical rivet row occurred either more or less widespread and crack propagation remained then concentrated around the cracked holes until panel failure (without linking up of cracks) or at two or more rivets positioned close together (but not necessarily next to one another) resulting in more cracks growing simultaneously and linking up of these cracks during test continuation. The former behaviour generally occurred in the uniaxial tests, the latter in the biaxial tests.  
In some uniaxial tests crack initiation in the critical row was not found at all.
- iv) As a consequence of the large continuous crack (= crack extending over one or more rivet spacings) being present in the critical rivet row at the moment of panel failure (see iii)) all biaxially tested panels failed in mode A (67%) or in mode C (33%); see Figure 5. On the contrary the uniaxially tested panels generally failed in mode B (60%) because no cracks or very small continuous cracks had developed in the critical rivet row during the test. However, sometimes despite this fact uniaxial panels still failed in mode A (20%) or mode C (20%) because during the test no cracks or rather small cracks had developed at the tear strap ends.
- v) During the tests generally cracks initiated at the tear strap ends from the rivet holes in the skin due to secondary bending in these areas. Propagation of these cracks was stopped during the test by applying a "ball-indentation" (BI) process in the crack tip region (see text). This crack arresting process had to be repeated a number of times during the test continuation because new cracks initiated at other locations or reinitiation of cracks at the hammered crack tips occurred. The objective of the application of the BI-process was to retard crack propagation at the tear strap ends to such an extent that cracks in the critical row meanwhile would have a chance either to initiate or to propagate with the consequence that panel failure still might occur across the critical rivet row. In this respect the application of the BI-process appeared to be more effective in the biaxial tests than in the uniaxial tests.

- vi) It was found from the inspections carried out during the tests that in the panels that failed in mode A or mode C the last inspections at which still separate cracks at rivet holes were found to be present generally were at levels above 95% of the panel failure lives. Consequently, development of these cracks across the rivet row, ultimately leading to panel failure across the cracked row, occurred in less than 5% of the panel lives.

#### REFERENCES

1. A laboratory study of multiple site damage in fuselage lap splices, ADL report (Draft version) written by Ronald A. Mayville and Milton R. Sigelmann, February 1992.
2. Evaluation of the newly developed NLR biaxial test specimen, NLR report CR 90268 C written by G.J. de Jong, July 1990.

Table 1  
ADL/FTI uniaxial fatigue tests on riveted lap joints

Parameters considered	Levels selected	
	original programme 1)	additional tests 2)
stress level (ksi)	12 (14) and (16)	14 18 and 20
rivet type	(flush head) + Briles	<u>flush head</u>
rivet spacing (inches)	(.75) (1.0) and 1.29	<u>1.0</u>
rivet orientation	(continuous) + staggered	<u>continuous</u>
number of rivet rows	(3) + 5	<u>3</u>
skin thickness (inches)	.040 (.050) and .063	.040 .063 and .080
number of specimens	51	21

- 1) the encircled values are chosen for the NLR testing programme  
2) the underlined levels pertain to the baseline design

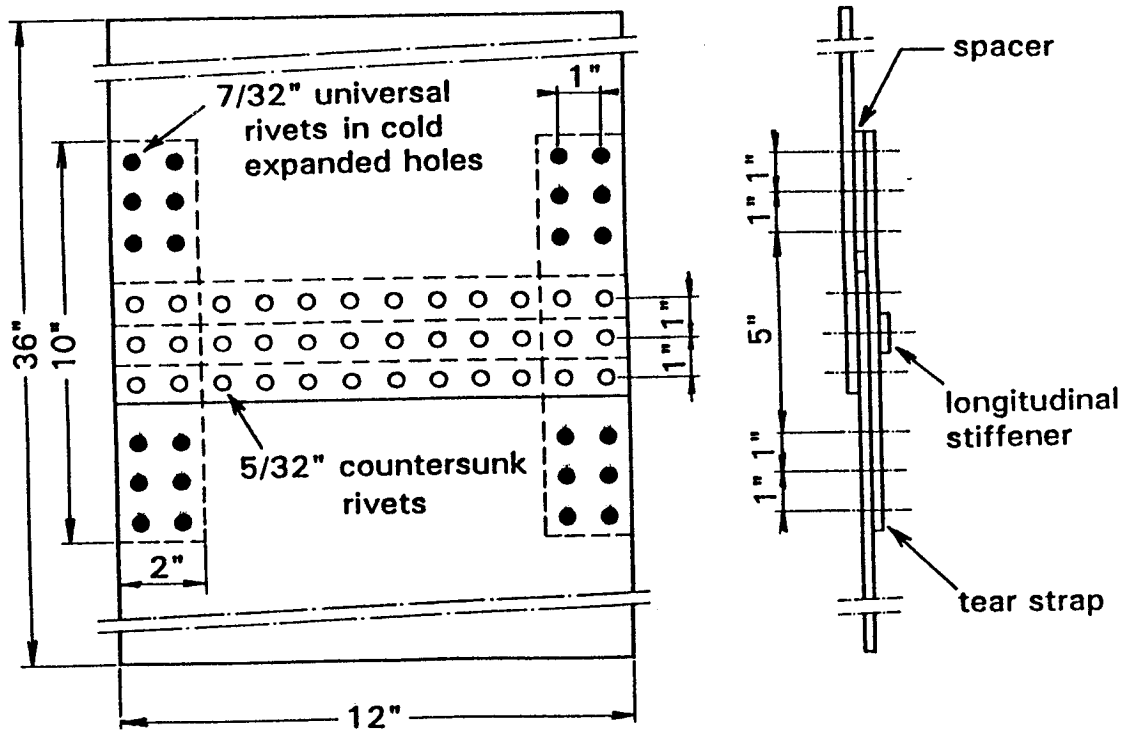
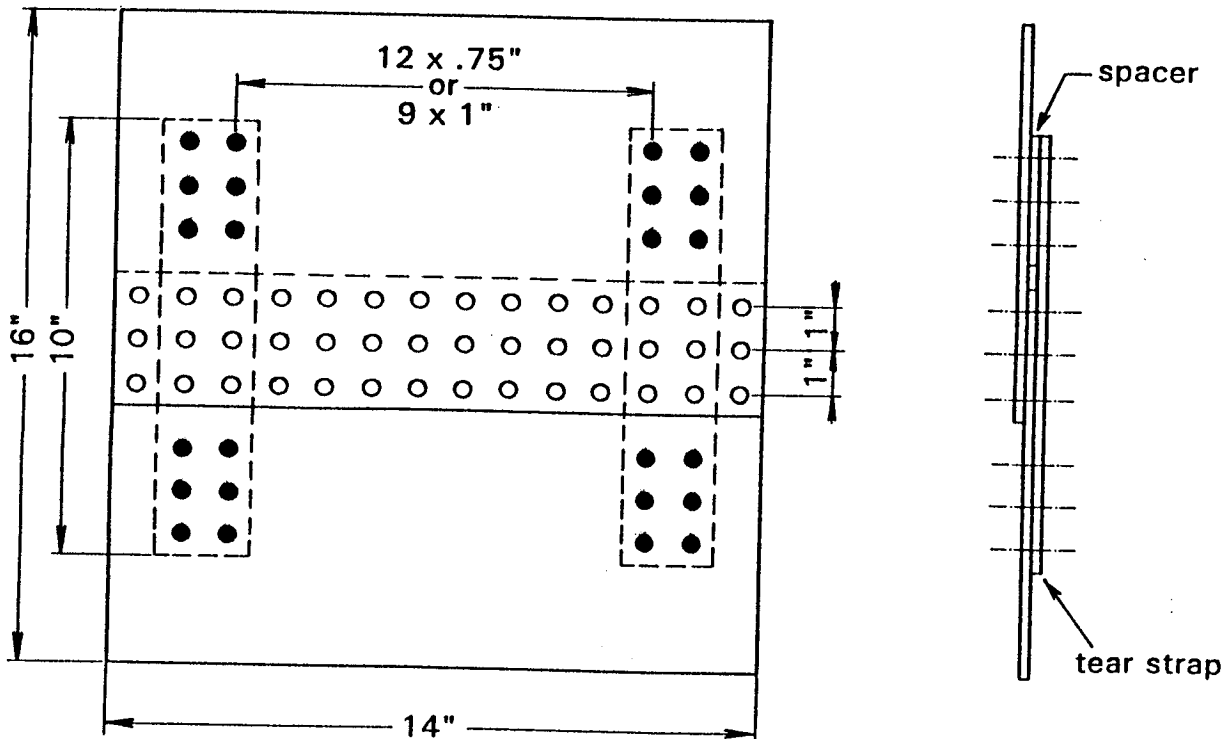


Fig. 1 Geometry and dimensions (inches) of specimens (baseline design)

Table 2  
NLR test matrix

Specimen group no 1)	$\sigma_{max} = \sigma_H$ (ksi) 2)	rivet spacing (inch)	skin thickness (inch)
1	14	1.0	0.05
2		.75	
3	16	1.0	
4 3)		.75	

- 1) Two repeats for uniaxial tests, three repeats for biaxial tests
- 2)  $\sigma_H$  = hoop stress,  $\sigma_L$  = longitudinal stress, in biaxial tests:  $\sigma_L/\sigma_H = 0.5$
- 3) Only in this group of specimens uniaxial tests were carried out both with and without a longitudinal stiffener (was present in all ADL/FTI specimens)



note: All specimens were delivered with a length of 36 inches.  
The biaxial specimens were shortened to 16 inches.

Fig. 2 Geometry and dimensions (inches) of biaxial specimens tested by NLR

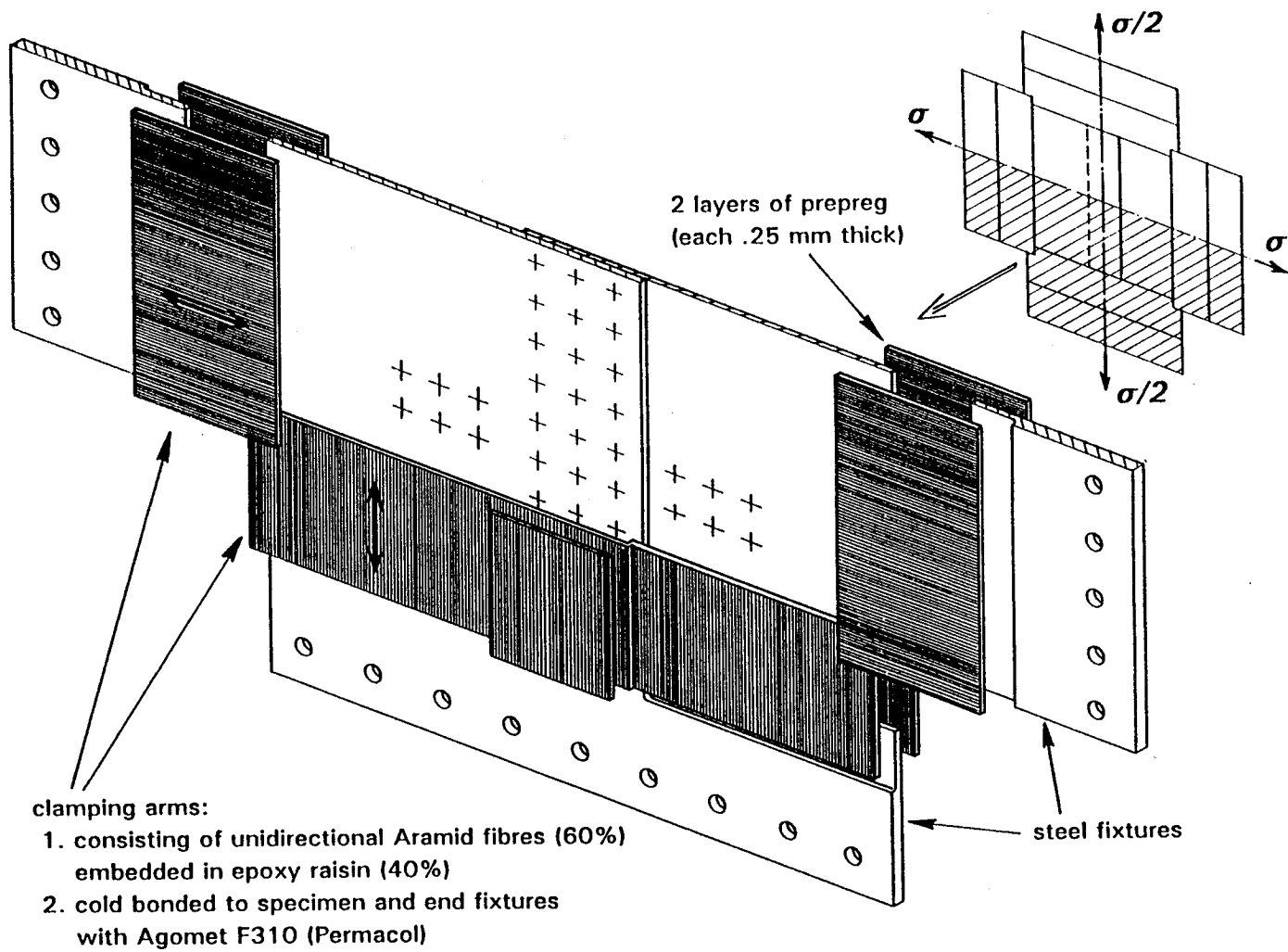


Fig. 3 Exploded view of biaxial lap joint specimen  
(half specimen drawn)

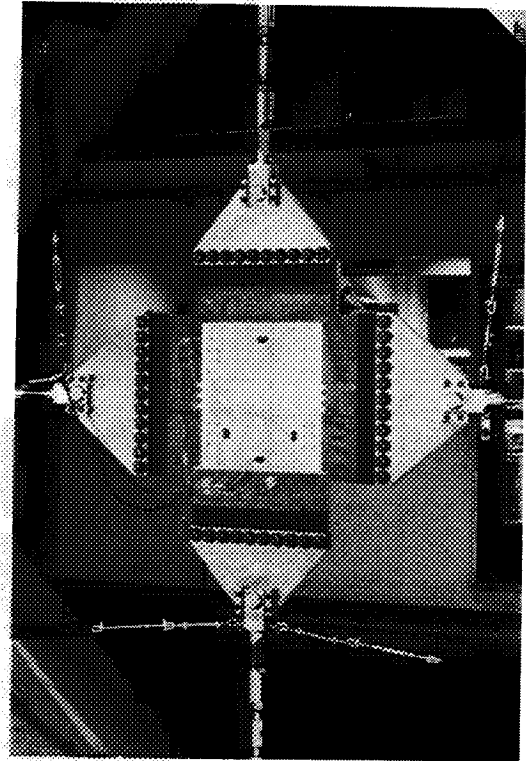
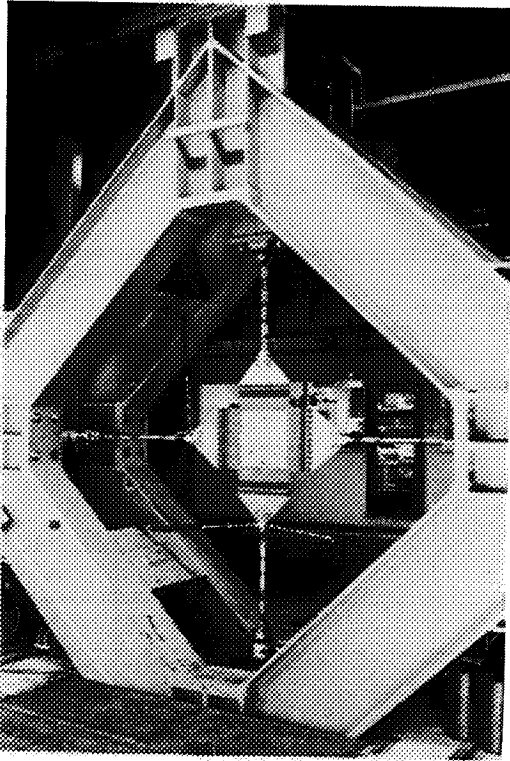


Fig. 4 Biaxial specimen mounted in test frame

**Table 3**  
**Survey of uniaxial and biaxial fatigue test results**

notes: 1 the results in the shaded areas refer to biaxial tests  
2 the values in parentheses represent percentages of panel failure lives

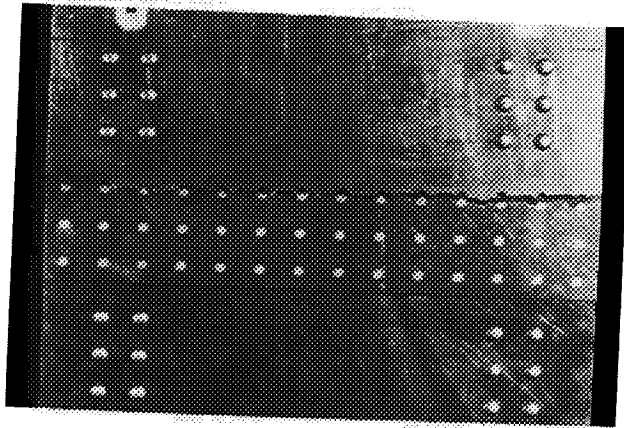
$\sigma_{max}$ (ksi)	rivet spacing (inch)	specimen identification no		first crack(s) in skin (kcycles)			life until panel failure (kcycles)	failure mode 2)
				at critical (countersunk) rivet row 1)	at tear strap ends			
					LHS	RHS		
group	no							
14	1.0	1a-	A	475 (83)	393 (69)	566 (99)	570	A
			B	613 (89)	525 (76)	525 (76)	691	C
			C	220 (75)	295(100)	-	295	A
		1b-	A	50 (25)	-	-	204	A
			B	120 (55)	-	-	218	A
	.75	2a-	A	485 (85)	485 (85)	-	573	C
			B	750 (63)	475 (40)	900 (75)	1195	C
			C	600 (67)	468 (52)	-	893	A
		2b-	A	120 (18)	357 (53)	470 (70)	672	B
			B	690 (93)	450 (61)	635 (86)	742	B
16	1.0	3a-	A	313 (87)	325 (90)	-	359	A
			B	363 (89)	215 (53)	409(100)	410	A
			C	250 (85)	290 (98)	-	295	A
		3b-	A	230 (78)	260 (88)	-	295	C
			B	120 (36)	300 (90)	270 (81)	334	B
	.75	4a-	A	430 (87)	225 (46)	380 (77)	490	A
			B	475 (92)	413 (80)	488 (95)	515	C
			C	425 (87)	303 (62)	335 (69)	488	A
		4b-	A	281 (89)	175 (56)	254 (81)	315	B
			B	-	263 (62)	342 (81)	422	B
		4c- 3)	A	400 (96)	245 (59)	253 (61)	416	C
			B	-	216 (75)	270 (94)	288	B

1) crack initiation defined by: cracks  $\geq 0.5$  mm at more than one rivet  
or crack  $> 1$  mm at a single rivet

2) panel failure modes: mode A = across critical rivet row  
mode B = across tear strap ends  
mode C = combination of modes A and B

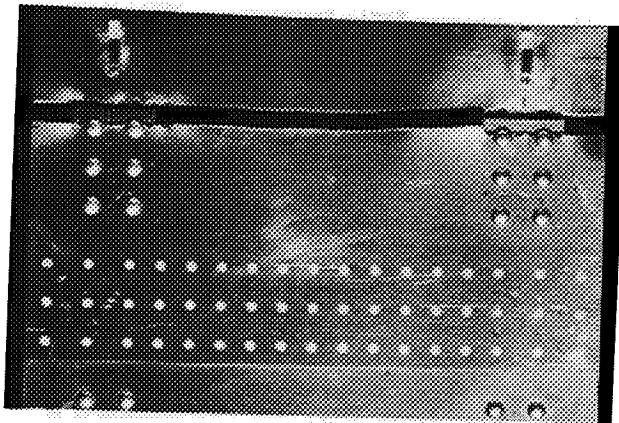
3) specimens provided with longitudinal stiffener (similar to panels tested by ADL/FTI)

**Mode A**



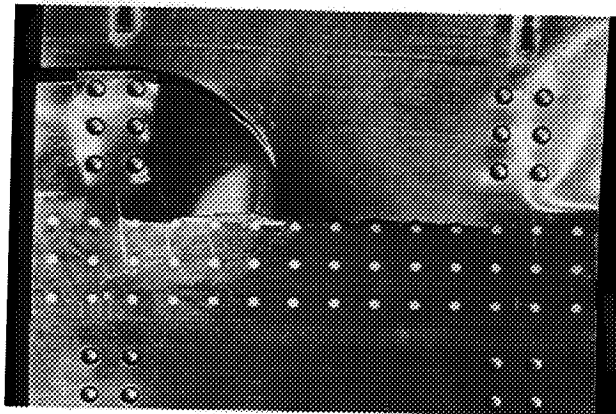
panel: 1b-A  
failure: 204 kcycle

**Mode B**



panel: 4b-A  
failure: 315 kcycles

**Mode C**



panel: 3b-A  
failure: 295 kcycles

Fig. 5 Panel failure modes

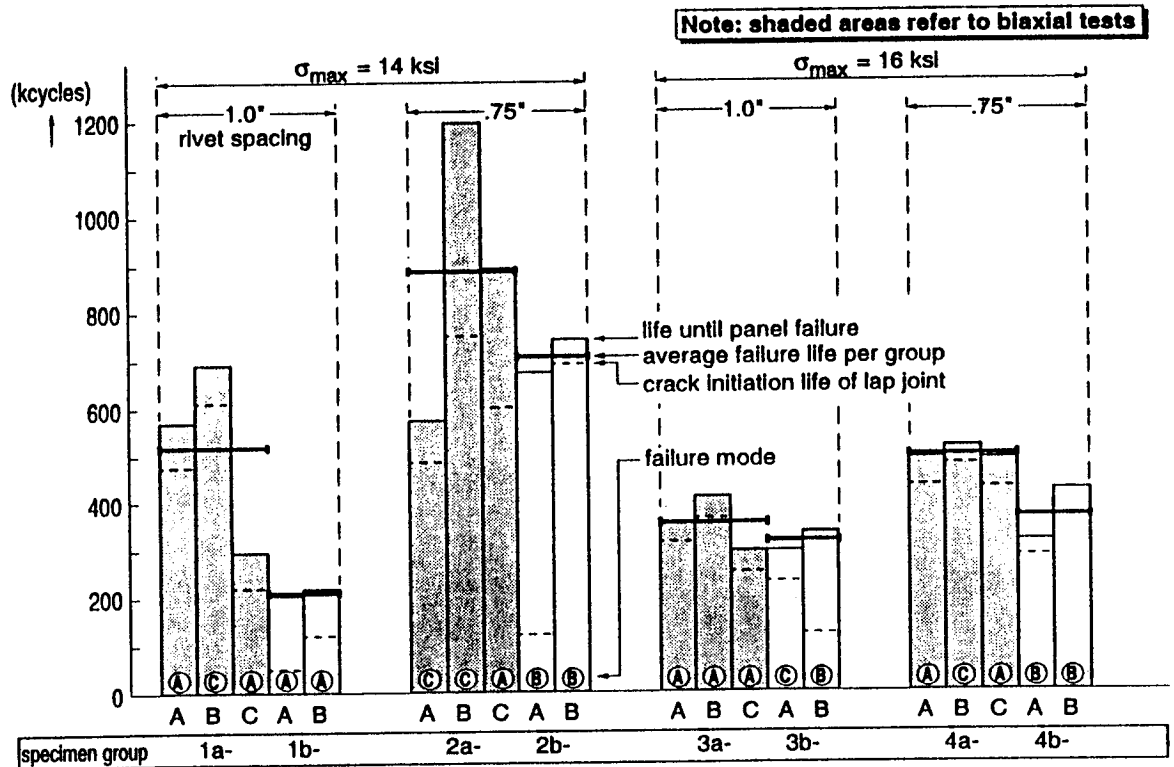


Fig. 6a Crack initiation in lap joints and panel lives until failure (data taken from Table 3)

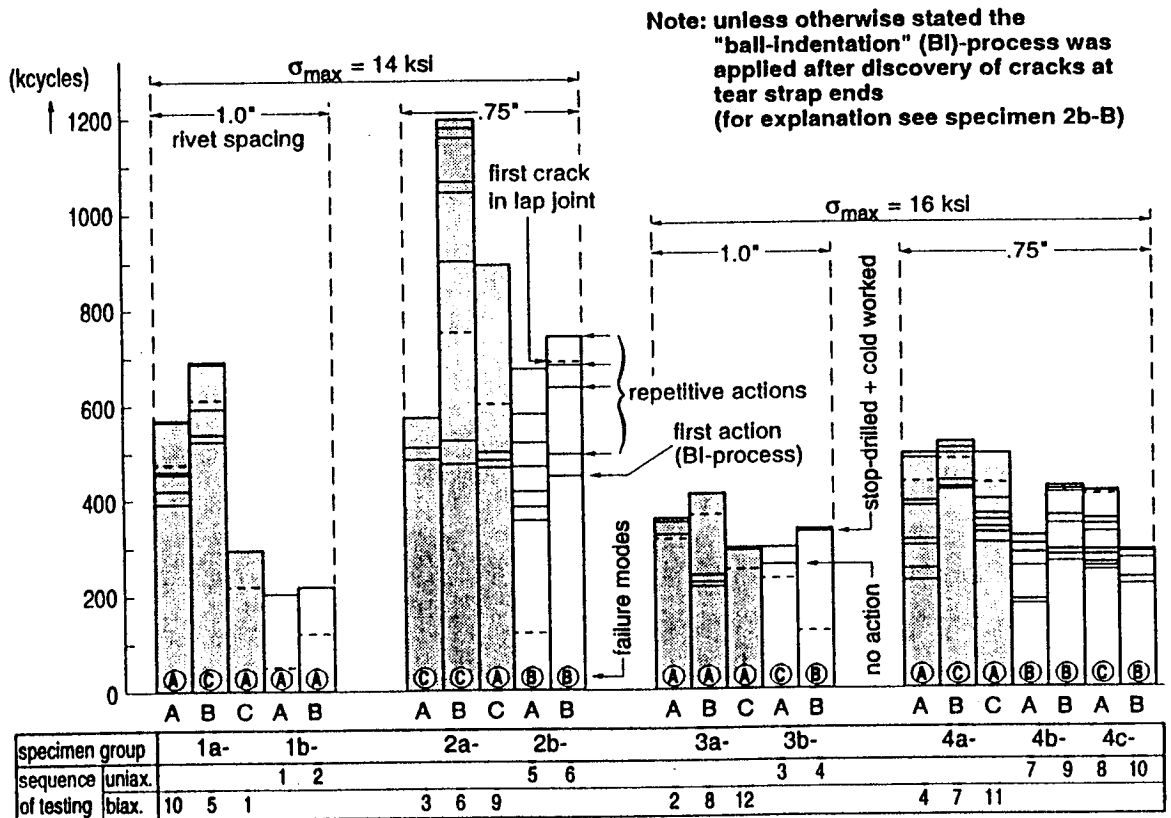


Fig. 6b Crack initiation at tear strap ends and corrective actions taken

Notes: 1. \* = crack indication

2. Crack lengths are measured from countersunk rivet heads

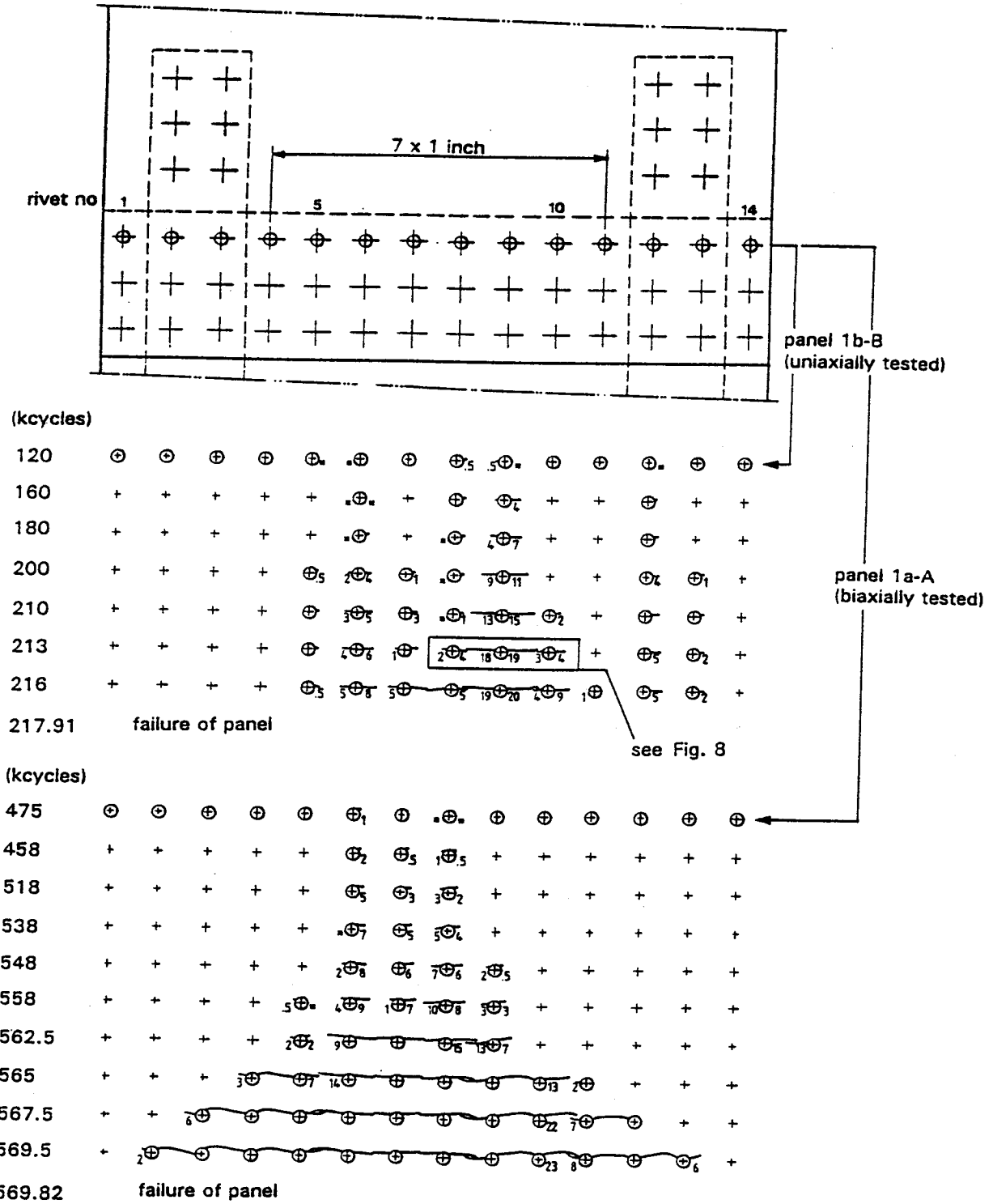


Fig. 7 Crack initiation and propagation in critical rivet row for uniaxial and biaxial specimens (typical)

\* photograph is taken after 213 kcycles } see Fig. 7  
\* panel failure after 217.91 kcycles

rivet nos:

8

9

10

critical row

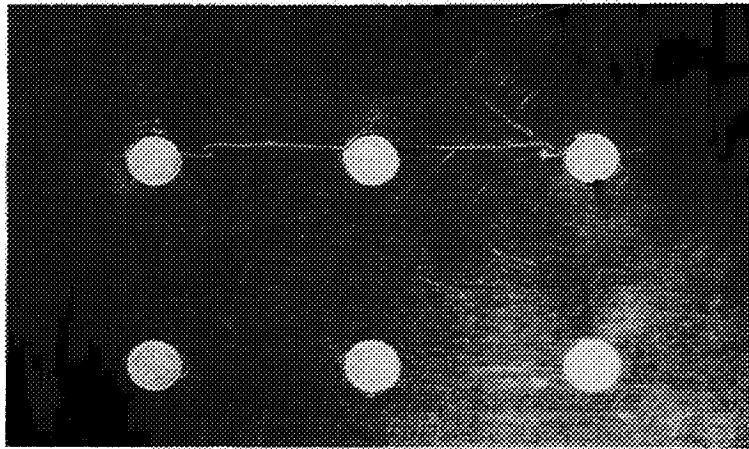


Fig. 8 Photograph of cracks in uniaxially tested specimen 1b-B

Table 4  
Crack lengths in skin just before failure + failure modes

$\sigma_{max}$ (ksi)	rivet spacing (inch)	specimen identification no		life until panel failure (kcycles)	failure mode	present just before panel failure		
		group	no			continuous crack in critical row (no of rivet spacings)	crack length at tear strap ends (mm) 1)	
							LHS	RHS
14	1.0	1a-	A	570	A	11	30	14
			B	691	C	10	48	42
			C	295	A	12	33	none
		1b-	A	204	A	2	none	none
			B	218	A	3	none	none
		.75	2a-	A	573	C	13	53.5
	B			1195	C	9	27.5	22
	C			893	A	8	26.5	none
	2b-		A	672	B	none	55.5	39
		B	742	B	none	69.5	16.5	
16	1.0	3a-	A	359	A	12	75	none
			B	410	A	11	24.5	12
			C	295	A	11	13.5	none
		3b-	A	295	C	6	29 2)	none
			B	334	B	none	57.5 3)	57 3)
		.75	4a-	A	490	A	13	30.5
	B			515	C	9	29.5	15
	C			488	A	14	30.5	28
	4b-		A	315	B	2	57.5	42
			B	422	B	none	46	29.5
	4c-		A	416	C	2	47	38.5
			B	288	B	none	53	16

1) unless otherwise stated, these cracks were stopped by applying the "ball indentation" process (see text)

2) no actions taken after discovery of cracks

3) cracks stop-drilled ( $\varnothing$ 5 mm and holes cold worked)

**Table 5**  
Development of MSD during the last part of the test

specimen number	separate cracks present at		number of kcycles at which a continuous crack was found														failure (kcycles)	
	kcycles	no. of rivets	length of crack found (expressed in number of rivet spacings)															
			1	2	3	4	5	6	7	8	9	10	11	12	13	14		
1a-A	557.5 (97.8)	5		562.5 (98.7)				565 1+4		567	567.5 7+1	568.5 8+1	569 8+2	569.8				569.82
1a-B	675 (97.8)	3	683 (98.9)															690.5
1a-C	277.5 (94.1)	3	279 (94.6)	284 1+1		287 3+1	288 4+1	289 4+2	290			291	293	294	295			295
1b-A	180 (88.4)	6		200 (98.2)														203.64
1b-B	215 (98.7)	5	216 (99.1)					216.5						216.9				217.91
2a-A	522.5 (91.1)	2	537.5 (93.8)		562.5 1+2			567.5						572.5		573.2		573.27
2a-B <sup>1)</sup>	1137.5 (95.2)	2	1150 (96.2)	1163					1193	1194	1195							1194.85
2a-B <sup>2)</sup>	1175 (98.3)	3		1183 (99)	1188			1193			1195							
2a-C <sup>2)</sup>	875 (98)	3			885 (99.1)	887.5			890	892.5	893.2							893.18
3a-A	355 (98.8)	4						356 (99.1)			357	357.5		358.5	359			359.17
3a-B	400 (97.7)	3			406.3 (99.2)	407.5					408		408.5	409.5				409.5
3a-C	285 (96.6)	4	287.5 (97.5)	290	291.3 2+1			292	292.3	292.8	293	293.5	294.3	294.8				294.88
3b-A	285 (96.7)	2	288 (97.7)	289.6	292	293.5			294.6									294.81
4a-A	475 (96.9)	4	480 (97.9)	485				487.5			488.5	489	489.5		490	490.4		490.44
4a-B	508.5 (98.7)	4		511.5 (99.3)					513	513.5	514	514.5						515.33
4a-C	462.5 (94.9)	4	470 (96.4)	477.5							485 4+4		485.5 5+5	486 6+5	487 6+6	487.3 7+6	487.5	487.57
4c-A	412 (98.9)	7		416 (99.9)														416.39

Notes: 1. The shaded areas pertain to biaxial specimens

<sup>1)</sup> cracks in critical countersunk rivet row

<sup>2)</sup> cracks in critical formed head rivet row

2. The values in parentheses represent percentages of panel failure lives

3. Unless otherwise stated the cracks were present in the critical countersunk rivet row

4. Only results of specimens that failed in mode A or mode C are presented

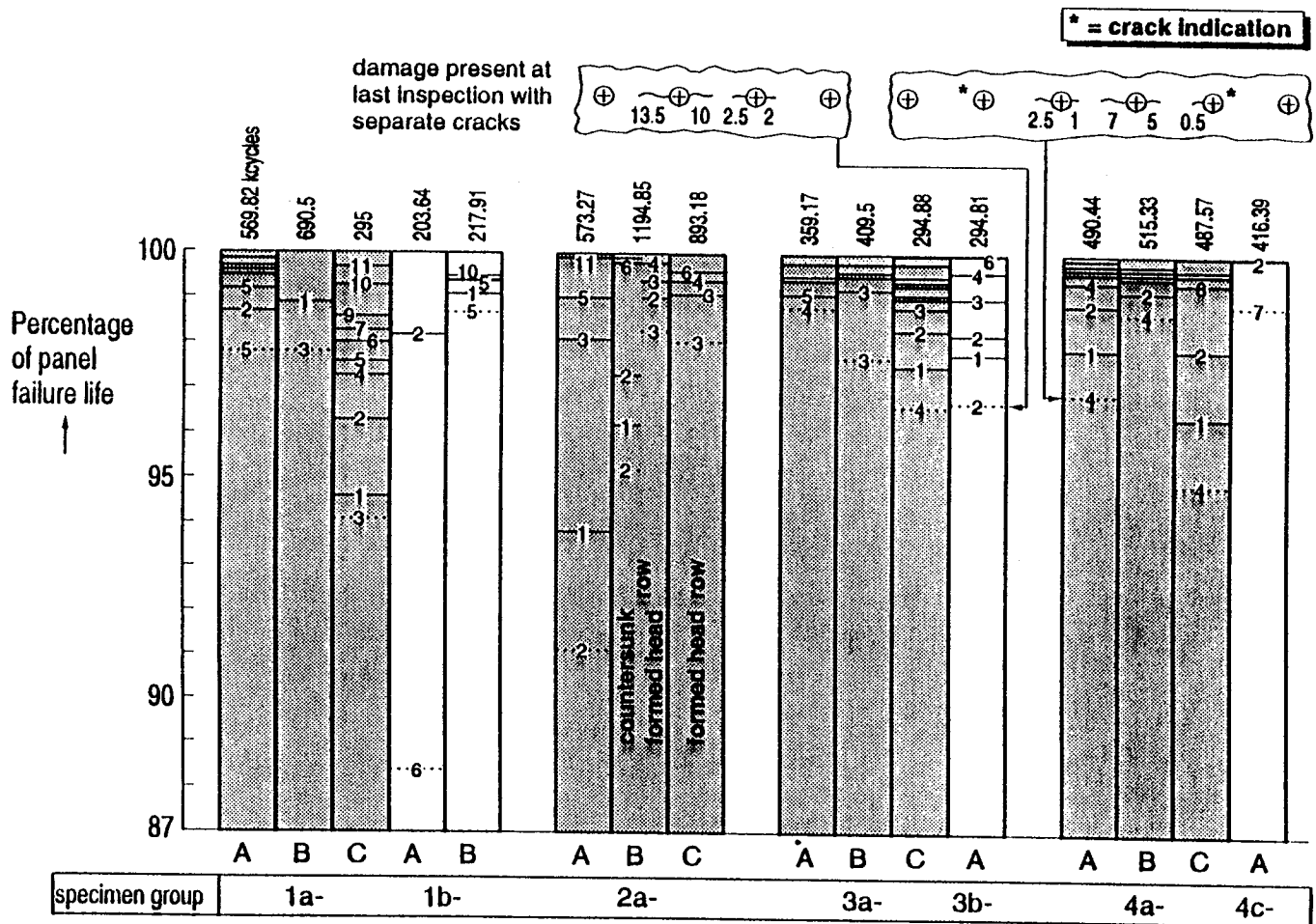


Fig. 9 Development of MSD after the last inspection with separate cracks